Journal of Agricultural Science and Technology (JAST), 28(1)
In Press, Pre-Proof Version

Pedogenesis and clay mineralogy of a climolithotoposequence in Jazmurian Watershed, central Iran

Saleh Sanjari[1], and Mohammad Hady Farpoor[1]*

Abstract

Topography, parent material, and climate are critical factors influencing pedogenesis and the clay mineralogy of soils. There is a paucity of data regarding the soils and sediments of the Jazmurian Watershed in south-central Iran. This study selected various landforms, including rock and mantled pediments, alluvial fans, piedmont plains, lowlands, and playa, characterized by igneous and sedimentary parent materials and situated within aquic, xeric, and aridic soil moisture regimes, to investigate soil genesis and clay mineralogy in the region. The findings indicated that the most significant soil development occurred on rock and mantled pediments, as well as on older alluvial fan sediments, in contrast to the less developed soils found on younger alluvial fan deposits. The clay minerals identified through X-ray diffraction (XRD) analyses included smectite, illite, chlorite, palygorskite, and kaolinite. The presence of palygorskite in the sedimentary soils was attributed to inheritance from the parent material, while in soils derived from igneous parent material, palygorskite was formed through pedogenic processes. Pedogenic features associated with calcium carbonate, such as coatings, infillings, and nodules, as well as clay coatings and infillings, were observed in both aridic and xeric soil moisture regimes. The occurrence of clay pedogenic features in the arid regions of the watershed may suggest a historical paleoclimate with greater moisture availability. Conversely, lenticular shapes, interlocked plates, and gypsum infillings were exclusively noted in the arid regions and lower elevations of the watershed, reflecting the current arid climate. The study established a strong correlation between soil formation and the factors of climate, parent material, and relief within the area.

Keywords: Central Iran, Geomorphic surface, Paleoclimate, Paleosols, Soil evolution.

1. Introduction

Soil formation and evolution influenced by soil-forming factors have been the focus of many pieces of research (Badia et al., 2020; Owliaie et al., 2018; Wilson et al., 2017; Yousefifard et al.,

[1] Department of Soil Science, Faculty of Agriculture, Shahid Bahonar University of Kerman, P.O. Box: 76169-14111, Kerman, Islamic Republic of Iran.
* Corresponding author; e-mail: farpoor@uk.ac.ir

2015, Farpoor et al., 2012, Moazallahi and Farpoor, 2012; Saez et al., 2003). Soil genesis related to geomorphology helps better understanding of soil forming factors and processes (Moghbeli et al., 2019; Sanjari et al., 2011). Owliaie et al. (2018) reported the impact of parent material and geomorphic position on physicochemical properties, clay mineralogy, and micromorphology of soils, south western Iran.

Lithology, together with other soil forming factors is reported as a major factor affecting pedogenesis (Wilson et al., 2017). Soil characteristics in northwest Iran affected by volcanic and plutonic rocks were studied by Yousefifard et al. (2015). They found more evolution in soils derived from volcanic rocks compared to plutonic ones. Soil properties and evolution were mainly affected by particle size and mineralogy of parent material in soils of arid Kapehdagh Basin, northeast Iran, which is an emphasis on the relationship between soil and parent material in that area.

Climate has a major role on the weathering processes of parent material. Climatic variations influence on the type and the rate of soil forming processes which in turn affect physicochemical properties and clay mineralogy of soils (Phillips et al., 2008). Weathering is highly related to the climate and trioctahedral minerals such as mica and chlorite may transform to dioctahedral smectite due to the high rate of weathering (Egli et al., 2008). Soil evolution in Nevada was affected by weathering rate and moisture regime (Elliot and Dorhan, 2009).

Soil minerals could be used to understand soil genesis (Graham and O'Geen, 2010), manage arid and wet land soils (O'Geen et al., 2008), and interpret paleo environmental conditions (Sanjari et al., 2012; Monafi, 2010; Khormali and Abtahi, 2003). Clay mineralogy of soils in Jiroft area, central Iran showed that due to high water table, palygorskite stability decreased and smectite dominated in soils from mantled pediment toward alluvial plain (Sanjari et al., 2011). In a soil geomorphology study of the southern parts of central Iran, Sarmast et al. (2017) reported chlorite, smectite, illite, palygorskite, and kaolinite clay minerals on different geomorphic positions.

Micromorphology is a useful complementary tool for soil morphology and evolution studies and seems necessary to better classify and manage soils of an area (Stoops, 2003). In a soil geomorphology study of Sirjan Playa, central Iran, Farpoor et al. (2012) reported calcite coatings and infillings in pediments, but lenticular shape and interlocked plates of gypsum in piedmont plain and playa landforms. Clay coating and infilling in the piedmont plain was attributed to the more available humidity of the climate in the past by the same researchers. Soil micromorphology related

to geomorphic position in central Iranian soils was studied by Sarmast et al. (2019). They reported clay (coating), calcite (nodule, coating, quazicoating, and infilling), anhydrite (nodule), gypsum (lenticular, vermiform, and interlocked plates), and halite (coating) pedo-features in the area under study.

Sixty watersheds were investigated in a study conducted by Krinsley (1970) in central Iranian plateau and Jazmurian is among the most widespread playas reported in that report. Limited data about soils and environmental factors in this playa are available. The only published report dates back to the study on sediments of the area related to geomorphic positions using aerial photo interpretations and limited field studies (Krinsley, 1970). Since climate, parent material, and geomorphic position are hypothesized to affect soil genesis and evolution on one hand, and limited data on soils of the study area are reported from the other hand, the present research was conducted with the following objectives: to study 1) physicochemical soil properties, clay mineralogy, and soil micromorphology in soils of the area, 2) the origin and distribution of clay minerals related to the variation of soil forming factors, 3) soil development along a climotopolithosequence.

2. Materials and methods

2.1. Study area

Jazmurian Watershed as a part of central Iran, Makran, and southeast Iran zones located in Kerman and Sistan-Baluchestan Provinces (56° E to 62° E and 26° N to 30° N) was selected as the study area (Fig. 1). The maximum elevation in the area is 4400 m above sea level (asl) for the Shah Mountain, Rabor area and the minimum elevation is only 360 m (asl) at Jazmurian Playa. Two main rivers including non-saline Halilrood which heads from Kerman Province elevations (north of the watershed) and saline Bampoor which heads from Iranshahr elevations (east side of the watershed), both end to central lake of Jazmurian Playa (Fig. 1). Jazmurian Playa is a depression of Late Pliocene Era (Namaki 2003). Miocene faulted rocks and evaporites of Upper Red Formations are at the east boundary of the watershed. Jebalbarez igneous mountain (granite, diorite, and andesite) is located at north. Intrusive and external igneous rocks are reported at the west and southeast sides of the area and the Beshagard Paleocene and Cretaceous Ophiolite Mountains together with Mokran colored Melange which separate the watershed from Oman Sea are located at the south (Mohammadi, 2011). Soil mean temperature varies from 13.1 °C in Rabor and Hanza (Mesic soil temperature regime) to 28.9 °C in Iranshahr and Dalgan areas (Hyperthermic soil

temperature regime). Mean Annual precipitation also varies from 287 mm in Rabor and Hanza (Xeric moisture regime) to 82 mm in Roodbar Jonoub areas (Aridic soil moisture regime).

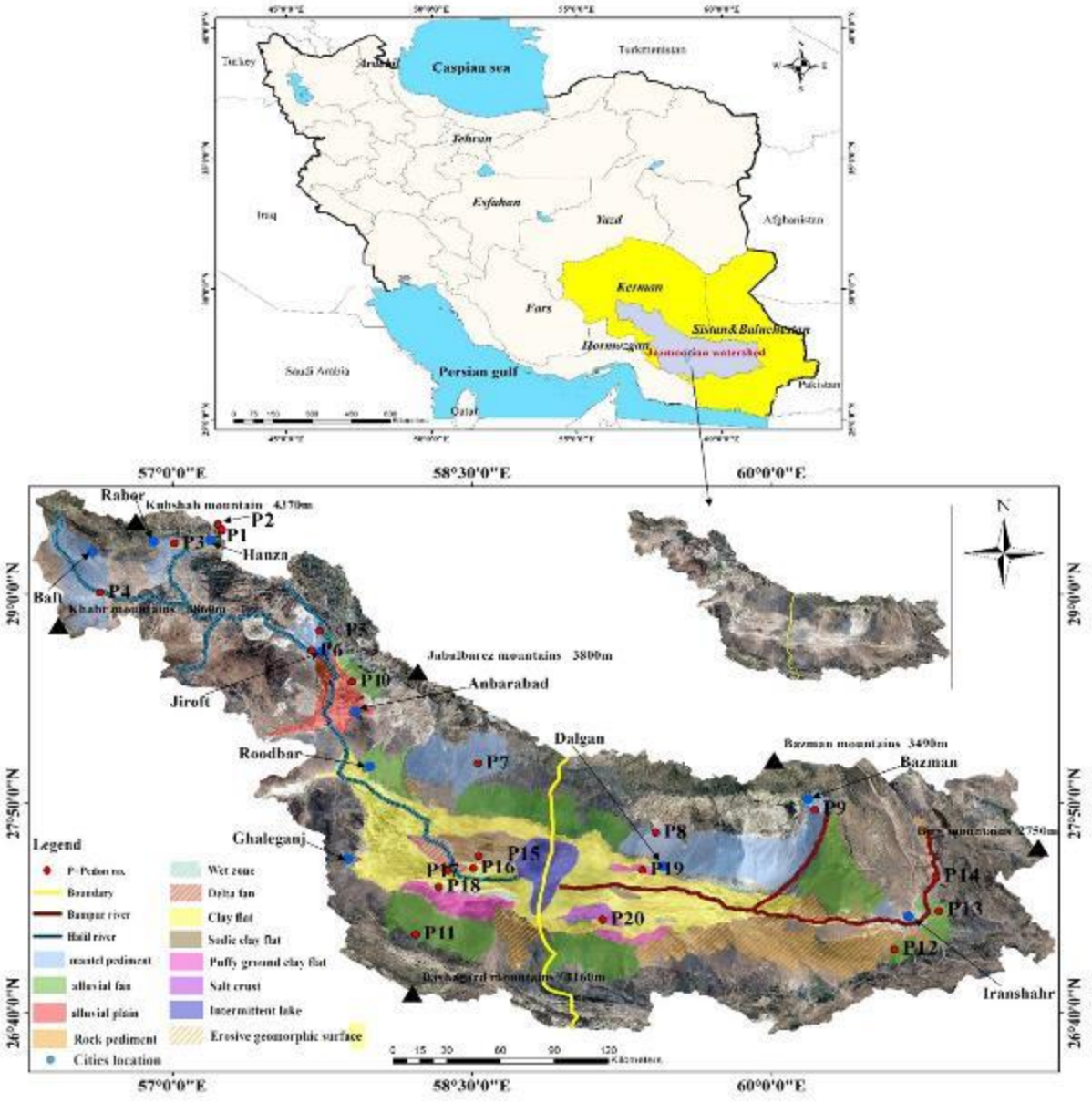

Fig. 1. The study area, geomorphology map showing location of representative pedons.

2.2. Field studies

Alluvial fan, rock and mantled pediments, Piedmont plain, playa, and lowland were among dominant landforms studied after detailed field and aerial photo observations (Fig. 1). Playa was also divided to clay flat, sodic clay flat, puffy ground clay flat, salt crust, wet zone, fan delta, and lake geomorphic surfaces. Considering variations in elevation, soil moisture and temperature

regimes, and parent material, one representative pedon on each geomorphic surface (total of 20 pedons) were selected, described (Schoeneberger et al., 2012), and sampled. Fig. 1 shows the study area and the location of representative pedons.

Various soil moisture regimes included; xeric (pedons 1 and 3), aquic (pedons 2, 18) and aridic (other pedons) and temperature regimes included mesic (pedons 1, 3 and 4), thermic (9), hyperthermic (other pedons) related to elevation variations and the vast extent of the area were found (Banaie, 1998).

2.3. Laboratory investigations

After sampling, air-dried ground soil samples passed through a 2 mm sieve and the volumetric percentage of coarse fragments was determined. Particle size distribution was investigated using pipet method (Gee and Bauder, 1986). Jenway pH and EC meters were used to determine the pH of saturated paste and the EC of saturated extract, respectively. The sum of gypsum and anhydrite was analyzed using acetone precipitation (Nelson, 1982). Gypsum was investigated using the Oven method (Artieda et al., 2006). Anhydrite was calculated by the subtraction of gypsum from gypsum+anhydrire (Wilson et al. 2013). Back titration of excess NaOH by HCl was used for equivalent calcium carbonate determination (Nelson, 1982). Wet oxidation using potassium dichromate (Nelson and Sommers, 1982) was used for organic carbon determination. Substitution of sodium acetate by ammonium acetate pH=7 was the basis for cation exchange capacity (CEC) determinations (Bower and Hatcher, 1966).

Micromorphological study

Undisturbed soil samples were impregnated using a Vestapol resin with acetaeric acid as the hardener and cobalt acetate as the catalyst for micromorphological studies, under vacuum. A BK-POL petrography microscope in plain (PPL) and crossed (XPL) polarized lights was used for thin section observations and interpretations performed by the Stoops (2003) guideline.

Clay mineralogy

Soil samples were prepared (Jackson, 1975; Kittrick and Hope, 1963) for XRD analysis and four treatments including Mg-saturated, Mg-saturated and treated by ethylene glycol, K-saturated, and K-saturated and heated up to 550 ^{o}C performed on each sample. A Broker DH8 Advance diffractometer with Cu as the target at 40 kv and 30 mA with the scan speed of 0.02 degree per

second was used for XRD analyses. The area under first order peaks of Mg saturated-treated by ethylene glycol was used as the reference for semi-quantitative clay mineralogy (Jones et al., 1954). Besides, several bulk soil samples were mounted on Al stubs by a carbon glue, coated with gold, and observed by scanning electron microscope (XL 30 ESEM Philips) as a complementary to clay mineralogy investigations.

3. Results and discussion

Table 1 shows selected physiochemical soil properties and soil classifications based on Soil Taxonomy (Soil Survey Staff, 2022) system.

3.1. Piedmont Plain

Pedon 1 on this geomorphic position is about 3620 m above sea level (asl) with a xeric moisture regime affected by diorite derived parent material (Fig. 1). Mollic and cambic horizons were determined through field studies, but no calcic or gypsic horizon was found. Gleyic condition caused by textural differentiation was the reason an Oxyaquic Haploxeroll to be formed.

Smectite, illite, chlorite, and kaolinite clay minerals were found in the Bw1 horizon and R layer (Table 2) which are accounted as a proof of the inheritance origin of minerals from parent material (Yousefifard et al., 2015). Palygorskite was also found in the Bw1 horizon (Table 2, Fig. 3a). Since palygorskite was neither present in the parent material (Fig. 3b), nor were the environmental conditions in this pedon suitable for its formation due to relatively high precipitation, the detrital origin (aeolian source) in this geomorphic surface could be a plausible reason for palygorskite as also supported by other researchers (Sarmast et al., 2017; Singer, 1989).

3.2. Lowland

This geomorphic position with the elevation of 3570 m asl and an aquic soil moisture regime was also affected by diorite parent rock (Fig. 1). Pedon 2 on this surface with Histic and Cambic horizons showed gleyic properties. Water logging together with a cold climate inhibited organic matter decomposition that is why about 16% organic carbon with an intermediate decomposition in this pedon was accumulated and caused Histic Humaquepts to be formed.

Illite and kaolinite were the only clay minerals formed in this pedon (Table 2, Fig.3c). Transformation of smectite to kaolinite due to high precipitation rate and low pH (Table 1) in this pedon could not be neglected. This could be the reason why the highest kaolinite content was found

in this pedon. On the other hand, lack of palygorskite is attributed to high weathering rate and the mineralogy of parent material which lacks palygorskite (Moazallahi and Farpoor, 2012). Transformation of palygorskite to smectite is reported to take place at the annual rainfalls more than 300 mm (Paquet and Millot, 1972) as a support.

Pedons 1 and 2 have the same parent material but different geomorphology and soil moisture conditions. Since the soils formed on the two mentioned locations are different (Haplustolls vs. Humaquepts), it is clear that climate (xeric vs. aridic) and topography (piedmont plain vs. lowland) played an important role on soil genesis and development in the area compared to parent material (both diorite).

Table 1. Selected physical and chemical properties of studied pedons.

Horizon	Depth (Cm)	Sand (%)	Silt (%)	Clay (%)	RF (%)	pH	ECe (dS m^{-1})	CCE (%)	Gypsum (%)	Anhydrite (%)	OC (%)	SAR (mmol L^{-1})$^{0.5}$
Pedon 1, Piedmont plain, 3620 m a.s.l., Diorite, USDA: Oxyaquic Haploxerolls												
A	0-20	15.1	46.6	38.3	2	6.5	1.2	2.0	ng	ng	3.5	1.1
Bw1	20-45	19.1	50.6	30.3	7	6.0	0.7	1.0	ng	ng	1.2	1.6
Bw2	45-80	27.1	48.6	24.3	18	6.4	0.5	0.7	ng	ng	0.7	1.4
Bg	80-100	11.1	51.6	37.3	23	6.5	0.4	1.7	ng	ng	0.9	1.4
C	100-140	37.1	44.6	18.3	46	6.6	0.5	1.2	ng	ng	0.5	1.6
R	>140	-	-	-	-	-	-	-	-	-	-	-
Pedon 2, Low land, 3570 m a.s.l., Diorite, USDA: Histic Humaquepts												
Oe	0-15	25.1	51.1	23.8	-	5.6	1.5	1.0	ng	ng	16.0	1.0
A	15-30	45.1	24.6	30.3	23	5.8	0.8	1.0	ng	ng	2.3	1.1
Bg1	30-65	53.1	16.6	30.3	27	5.8	0.5	0.5	ng	ng	1.4	1.4
Bg2	65-110	65.1	14.6	20.3	18	5.1	0.6	0.75	ng	ng	0.5	2.0
Pedon 3, Mantled pediment, 2247 m a.s.l., Andesite, USDA: Calcic Haploxeralfs												
A	0-13	39.1	39.3	21.6	6	7.2	1.4	8.5	ng	ng	0.5	1.5
Btk	13-45	35.1	37.3	27.6	34	7.9	0.9	26.2	ng	ng	0.6	2.0
Ck	45-85	71.1	13.3	15.6	58	7.8	0.8	17.7	ng	ng	0.3	2.3
C	85-105	77.1	9.3	13.6	66	7.6	0.6	14.0	ng	ng	0.2	2.4
2Btk	105-145	7.1	65.3	27.6	-	7.7	0.6	15.0	ng	ng	0.1	2.5
2Bk1	145-175	23.1	58.6	18.3	-	8.0	0.7	24.0	ng	ng	0.1	3.0
2Bk2	175-215	11.1	68.6	20.3	-	7.9	0.7	44.2	ng	ng	0.1	3.4
Pedon 4, Mantled pediment, 1977 m a.s.l., Limestone, USDA: Typic Natrargids												
A	0-5	37.1	41.3	21.6	1	8.0	0.5	26.5	ng	ng	0.4	0.5
Btk1	5-35	23.1	39.3	37.6	-	8.3	1.2	28.7	ng	ng	0.3	6.2
Btk2	35-72	25.1	35.3	39.6	-	7.8	5.6	28.2	ng	ng	0.3	11.9
C	72-78	57.1	17.3	25.6	19	7.8	5.5	19.5	ng	ng	0.1	12.9
2Btnk	78-100	43.1	27.3	29.6	-	7.9	4.7	22.2	ng	ng	0.1	15.2
2Btnkk1	100-135	1.1	53.3	45.6	-	8.3	2.8	51.2	ng	ng	0.1	15.5
2Btnkk2	135-185	0	58.4	41.6	-	8.2	3.3	50.7	ng	ng	0.1	13.8
2Ckk	>185	0	89.4	10.6	-	8.0	3.6	88.9	ng	ng	ng	12.6
Pedon 5, Mantled pediment, 897 m a.s.l., Diorite, USDA: Calcic Argigypsids												
A	0-20	75.7	12.9	11.4	43	7.6	2.7	15.5	ng	ng	0.2	1.0
Btk	20-55	70.7	14.9	14.4	34	8.0	1.1	16.5	0.7	ng	0.2	1.4
By	55-85	89.7	1.9	8.4	69	8.0	1.3	14.5	5.2	ng	0.2	2.4
C	85-135	90.7	2.9	6.4	60	8.2	1.4	10.0	5.5	ng	0.3	1.2
Pedon 6, Mantled pediment, 860 m a.s.l., Diorite, USDA: Typic Natrargids												
A	0-20	51.4	17.0	31.6	5	7.6	1.6	20.0	ng	ng	ng	4.7

Btn1	20-65	41.4	16.0	42.6	-	7.6	8.2	19.5	ng	ng	0.1	16.5
Btn2	65-80	40.4	18.0	41.6	-	7.5	5.9	19.7	ng	ng	0.1	14.1
Btn3	80-125	39.4	20.0	40.6	-	7.6	5.2	20.5	ng	ng	0.1	13.3
C	125-140	79.4	9.0	11.6	84	7.8	2.4	20.2	ng	ng	0.1	5.7
2Btk	140-170	61.4	15.0	23.6	52	7.8	2.0	20.5	ng	ng	0.1	5.1
2Ck	170-200	85.4	6.0	8.6	72	7.9	1.3	21.2	ng	ng	0.1	2.5
Pedon 7, Mantled pediment, 615 m a.s.l., Diorite, USDA: Typic Haplogypsids												
A	0-10	67.1	16.6	16.3	55	7.4	8.0	11.7	0.6	3.8	0.1	4.3
By1	10-25	79.1	10.6	10.3	49	7.5	4.8	8.7	0.8	13.4	0.1	3.0
By2	25-50	81.8	6.6	11.6	45	7.6	2.9	4.2	23.0	2.7	ng	1.1
By3	50-80	81.8	8.6	9.6	56	7.6	2.9	3.5	14.1	ng	0.1	1.3
By4	80-120	79.8	6.6	13.6	56	7.7	2.9	3.0	14.0	ng	0.1	1.3
Bym	120-150	81.8	4.6	13.6	76	7.4	3.0	4.2	17.3	ng	ng	1.4
Bty	150-180	73.8	4.6	21.6	54	7.6	3.0	3.2	5.5	ng	0.1	1.5
Pedon 8, Mantled pediment, 490 m a.s.l., Andesite, USDA: Petrogypsic Haplosalids												
Horizon	Depth (Cm)	Sand (%)	Silt (%)	Clay (%)	RF (%)	pH	ECe (dS m^{-1})	CCE (%)	Gypsum (%)	Anhydrite (%)	OC (%)	SAR (mmol $L^{-1})^{0.5}$
A	0-10	55.8	33.3	10.9	21	7.4	43.5	37.7	0.7	ng	0.4	53.0
Bkyz1	10-35	47.8	41.3	10.9	24	7.1	140.5	27.2	2.0	17.4	0.4	64.5
Bkyz2	35-65	61.8	28.6	9.6	63	7.3	84.7	24.5	24.2	2.5	0.1	59.4
Bym	65-110	53.8	32.6	13.6	61	7.3	99.6	34.0	15.8	2.3	0.2	66.8
Bkyz	110-160	51.8	38.6	9.6	67	7.6	96.1	47.5	7.5	0.8	0.8	92.4
Ck	160-190	69.8	20.6	9.6	67	7.6	9.4	45.0	0.1	ng	0.1	7.0
Pedon 9, Mantled pediment, 860 m a.s.l., Diorite, USDA: Typic Natrigypsids												
A	0-15	79.1	8.6	12.3	22	7.7	5.6	8.2	ng	ng	0.1	14.4
Bk	15-40	76.5	15.3	8.2	26	7.4	9.2	16.0	ng	ng	0.1	11.4
Btk	40-55	56.5	25.3	18.2	35	7.3	25.5	16.2	0.6	ng	0.1	12.5
Btky	55-80	64.5	15.3	20.2	27	7.6	20.9	16.7	7.4	ng	0.1	11.3
Btnky1	80-140	66.5	15.3	18.2	34	7.6	19.8	15.5	5.8	ng	0.1	22.2
Btnky2	140-175	52.5	29.3	18.2	53	7.5	22.3	17.5	6.3	ng	ng	21.3
Pedon 10, Alluvial fan, 700 m a.s.l., young alluvial fan (Granite), USDA: Typic Torrifluvents												
A	0-15	91.4	3.0	5.6	40	8.1	0.5	4.0	ng	ng	0.5	1.0
C1	15-45	95.4	1.0	3.6	50	8.2	0.3	0.5	ng	ng	0.3	0.3
C2	45-75	96.4	1.0	2.6	51	8.2	0.3	6.5	ng	ng	0.1	0.2
C3	75-110	97.4	1.0	1.6	53	8.2	0.3	4.0	ng	ng	0.1	0.2
C4	110-145	97.1	1.0	1.9	74	7.9	0.3	3.7	ng	ng	ng	0.2
Pedon 11, Alluvial fan, 680 m a.s.l., old alluvial fan, USDA: Typic Calciargids												
A	0-30	39.8	24.0	36.2	50	8.0	0.6	8.7	0.1	ng	0.2	4.2
Btk	30-70	29.8	22.0	48.2	48	7.7	0.5	15.5	0.1	ng	0.1	7.9
Bk	70-110	75.8	14.0	10.2	60	8.1	0.7	18.0	0.2	ng	0.1	7.2
C	110-150	87.8	4.0	8.2	69	7.9	0.9	22.7	0.1	ng	0.7	6.1
Pedon 12, Alluvial fan, 635 m a.s.l., old Alluvial fan, USDA: Typic Haplocalcids												
A	0-30	72.4	18.6	9.0	5	8.2	0.7	9.0	ng	ng	0.1	4.6
Bk	30-55	78.4	12.6	9.0	38	7.7	3.1	12.7	ng	ng	0.2	7.5
C1	55-85	80.4	8.6	11.0	53	7.7	3.9	10.5	ng	ng	0.1	8.7
C2	85-110	88.4	2.6	9.0	72	8.0	2.3	11.7	ng	ng	0.2	8.1
C3	110-135	82.4	6.6	11.0	58	8.0	2.6	11.7	ng	ng	0.2	9.7
C4	135-165	62.4	12.6	25.0	83	8.1	2.2	11.7	ng	ng	0.1	14.4
Pedon 13, Alluvial fan, 632 m a.s.l., young Alluvial fan, USDA: Typic Torrifluvents												
A	0-5	80.4	10.6	9.0	51	7.7	0.8	9.0	ng	ng	0.1	0.8
C1	5-25	80.4	12.6	7.0	56	8.1	0.5	12.2	ng	ng	0.1	1.5
C2	25-40	86.4	4.6	9.0	64	8.1	0.5	12.5	ng	ng	0.1	0.9
C3	40-70	82.4	6.6	11.0	62	7.9	0.6	12	ng	ng	0.1	1.5
C4	70-90	68.4	14.6	17.0	77	7.8	0.8	12.5	ng	ng	0.2	3.2
C5	90-130	58.4	22.6	19.0	66	7.8	0.9	11.7	ng	ng	0.2	4.1
Pedon 14, Rock pediment, 793 m a.s.l., limestone, USDA: Typic Gypsiargids												

A	0-40	56.4	34.6	9.0	54	7.8	1.0	19.2	ng	ng	0.1	0.7
Btk1	40-80	50.4	34.6	15.0	43	7.8	0.8	20.0	ng	ng	0.2	1.2
Btk2	80-105	46.4	36.6	17.0	27	7.8	1.8	15.2	ng	ng	0.1	3.9
C	105-110	56.4	28.6	15.0	55	7.8	2.1	16.5	ng	ng	0.1	3.4
2Btk	110-125	48.4	36.6	15.0	4	7.6	3.6	21.0	0.1	ng	0.1	4.1
2Bty	125-150	43.0	38.3	18.7	3	7.6	3.5	10.7	24.0	ng	0.1	3.8
2Cy	150-170	64.5	25.3	10.2	53	7.7	3.8	14.0	17.6	ng	0.1	5.3
Pedon 15, Playa (sodic clay flat), 368 m a.s.l., Playa deposits, USDA: Typic Haplosalids												
Az	0-15	3.7	60.5	35.8	0	7.3	202.0	12.7	1.1	ng	0.7	359.9
Btnz	15-35	0.0	46.2	53.8	0	7.0	108.1	13.2	0.6	ng	0.4	117.5
C	35-50	0.0	84.2	15.8	0	7.2	60.2	17.5	0.2	ng	0.2	62.0
2Bz1	50-75	1.7	68.5	29.8	0	7.1	87.4	16.2	0.4	ng	0.2	121.2
2Bz2	75-110	13.7	60.5	25.8	0	7.5	58.1	16.5	0.3	ng	0.2	130.2
2Cz	110-145	9.7	78.5	11.8	0	7.9	24.5	18.2	ng	ng	0.1	111.9
Pedon 16, Playa (clay flat), 364 m a.s.l., Playa deposits, USDA: Typic Torriorthents												
A	0-20	8.4	64.6	27.0	0	8.3	3.2	16.2	ng	ng	0.3	67.8
C	20-60	20.4	70.6	9.0	0	7.7	11.1	16.5	ng	ng	0.1	46.8
2Cz	60-90	0.0	76.2	23.8	0	7.6	23.6	16.7	ng	ng	0.2	71.6
3Btnzb1	90-120	1.7	50.0	48.3	0	7.6	27.2	14.7	2.8	ng	0.2	77.3
3Btnzb2	120-150	9.7	42.5	47.8	0	7.7	32.1	14.0	3.1	ng	0.2	104.2
Pedon 17, Playa (fan delta), 378 m a.s.l., Playa deposits, USDA: Typic Torrifluvents												
A	0-20	32.4	46.6	21.0	0	7.5	1.8	13.0	ng	ng	0.2	4.5
C1	20-55	62.4	26.6	11.0	0	7.9	0.5	14.0	ng	ng	0.1	3.8
C2	55-85	2.4	60.6	37.0	0	8.3	1.2	16.7	ng	ng	0.1	11.0
C3	85-130	28.4	54.6	17.0	0	8.5	1.3	16.2	ng	ng	0.1	20.0
C4	130-160	50.4	36.6	13.0	0	8.4	1.0	14.7	ng	ng	0.2	16.5
Pedon 18, Playa (wet zone), 370 m a.s.l., Playa deposits, USDA: Typic Aquisalids												
Az	0-15	2.4	74.6	23.0	0	7.3	78.2	15.0	0.4	ng	0.5	189.5
Bz	15-30	8.4	70.6	21.0	0	7.5	57.3	16.0	1.2	ng	0.4	120.4
Btnz1	30-45	8.4	60.6	31.0	0	7.5	57.1	15.5	1.3	ng	0.5	118.7
Btnz2	45-95	0.0	71.0	29.0	0	8.2	43.3	15.5	0.6	ng	0.4	179.3
Bzg1	95-125	6.4	68.6	25.0	0	8.4	32.7	15.7	0.6	ng	0.3	151.7
Bzg2	125-170	30.4	48.6	21.0	0	8.1	30.2	17.0	0.5	ng	0.3	77.7
Pedon 19, Playa (clay flat with puffy ground), 374 m a.s.l., Playa deposits, USDA: Typic Haplosalids												
Az	0-30	0.4	47.3	52.3	0	8.3	92.7	11.5	4.8	ng	0.2	813.1
Bz1	30-60	4.4	45.3	50.3	0	8.2	70.6	11.7	4.3	ng	0.2	506.2
Bz2	60-90	0.0	67.7	32.3	0	8.2	99.4	11.0	1.7	ng	0.3	730.8
Bz3	90-135	0.4	59.3	40.3	0	8.3	69.8	13.0	0.5	ng	0.3	512.5
Bz4	135-155	14.4	51.3	34.3	0	8.2	49.5	13.0	ng	ng	0.2	330.6
Pedon 20, Playa (salt crust), 367 m a.s.l., Playa deposits, USDA: Typic Haplosalids												
Az	0-30	3.8	64.6	31.6	0	8.1	222.2	17.2	2.2	ng	0.4	1631.7
Bz1	30-60	1.8	60.6	37.6	0	8.2	138.4	18.0	0.9	ng	0.2	609.2
Bz2	60-90	5.8	58.6	35.6	0	8.0	78.1	15.5	2.0	ng	0.3	367.0
Bz3	90-120	15.8	48.6	35.6	0	8.0	51.4	15.5	1.7	ng	0.1	360.2
Bz4	120-155	17.8	52.6	29.6	0	8.0	35.6	15.0	2.3	ng	0.1	170.0

Horizon	Depth (Cm)	Sand (%)	Silt (%)	Clay (%)	RF (%)	pH	ECe (dS m^{-1})	CCE (%)	Gypsum (%)	Anhydrite (%)	OC (%)	SAR (mmol L^{-1})$^{0.5}$

174 ng: negligible, RF: rock fragment, ECe: electrical conductivity of soil saturated extract, OC: organic carbon, CCE:
175 calcium carbonate equivalent, a.s.l.: above sea level, SAR: sodium adsorption ratio
176
177
178

Table 2. Semi-quantitative mineralogical composition of clay minerals of soils and parent rocks in the studied area.

Landforms	Pedons	Parent materials	Soil moistures	Horizons	Smectite	Palygorskite	Illite	Chlorite	Kaolinite
Piedmont plain	1	Diorite	Xeric	Bw1	XXX	XX	XXX	ND	X
				R	XX	ND	XXX X	XX	X
Low land	2	Diorite	Aquic	Bg1	ND	ND	XXX XX	ND	XX
Mantel pediment	3	Andesite	Xeric	2Btk	XXXX	ND	XXX	ND	X
	4	Limestone	Aridic	Btk1	XX	XX	XXX	XXX	X
				2Ck	XX	XX	XXX	XX	X
	5	Diorite	Aridic	Btk	XXX	XX	XXX X	X	X
	6	Diorite	Aridic	Btn1	XXXXX	ND	XX	ND	X
				2Btk	XX	XX	XXX X	XX	X
	7	Diorite	Aridic	Bty	XXX	XX	XX	XX	X
	8	Andesite	Aridic	Bkyz1	XX	XX	XXX	XXX	X
	9	Diorite	Aridic	Btkyz	XXX	XX	XXX	XX	X
Rock pediment	14	Limestone	Aridic	Btk1	XX	XX	XXX X	ND	X
Playa	18	Playa deposit	Aquic	Bzn	XXX	XX	XXX	XX	X
				Btnz2	XXXX	ND	XXX	ND	X

Relative abundance of clay minerals is shown by: X: < 10 %; XX: 10-25 %; XXX: 25-50 %; XXXX: 50-75 %; XXXXX: > 75 %; ND: not detected.

3.3. Mantled pediment

Mantled pediment covers a vast area in the region. Soils in this landform were affected by igneous (pedons 3 and 8), diorite (pedons 5-7 and 9), and sedimentary limestone (pedon4) parent materials (Mohammadi, 2011) with two xeric and aridic soil moisture regimes. Argillic and calcic horizons were found in most pedons under study, but gypsic horizon was only found in the parts with an aridic soil moisture regime (Table 1). The argillic horizon (Fig. 2a) in the xeric parts of the area (pedon 3) could be due to the present humidity of the area, whereas argillic in other pedons with an aridic moisture regime, could only be attributed to the more available humidity of the past. Evidence of more humid paleoclimate in central Iran was reported by other researchers (Farpoor et al., 2012; Khormali et al., 2003; Khademi and Mermut, 2003).

Calcium carbonate equivalent (CCE) increased with depth (Table 1) in pedon 4 due to the presence of a calcareous parent material (about 89% in 2Ckk horizon). Besides, natric, salic, and

anhydritic horizons were also investigated in mantled pediment position. Anhydrite in pedons 7 and 8 was probably formed from dehydration of gypsum at the later stages of evaporation through evolution of the landform. High temperature caused this mineral to be preserved (Sarmast et al., 2017; Wilson et al., 2013).

Pedons 3 and 8 with the same parent material (andesite) showed different evolutions. Pedon 3 in the xeric part of the area had an argillic horizon, whereas no argillic was found in aridic parts with about 1800 m asl. Climate seems to be the only factor controlling soil evolution in these pedons. Pedon 3 is an Alfisol, but the other pedons were classified as Aridisols (Table 1).

Micromorphological observations showed clay (pedons 3-7 and 9), calcium carbonate (pedons 3-4 and 9), gypsum (pedons 5, 8-9), anhydrite (pedon 7), and compound (pedons 3 and 9) pedo-features (Fig. 2). Clay coating in pedon 3 (Fig. 2a) with a xeric soil moisture regime was probably formed in the present climatic conditions of the area. On the other hand, argillic horizon formation and clay coatings (Figs. 2 b, e, g, i, l, m) in other pedons in this landform with an aridic soil moisture regime could only be attributed to the presence of a more humid climate in the past. This was also supported by Farpoor et al. (2012), Sanjari et al. (2011), and Kademi and Mermut (2003) in Sirjan playa, Jiroft, and Isfahan arid areas of central Iran, respectively. A different clay coating in 2Btnkk1 horizon of pedon 4 was observed (Fig. 2c) which was affected by high Na content. This type of clay coatings was reported for the natric horizons where dispersion was induced by Na. The same results were also reported for saline and sodic soils of Fars Province by Khormali et al. (2003).

Calcite coatings were observed on the clay coatings in Btk horizon of pedon 3 (Fig. 2a) and Btky horizon of pedon 9 (Fig. 3m). The mentioned order of coatings in pedon 3 could be formed at the climatic situations of the present time, but for the pedon 9 is a proof of clay illuviation during more available humidity of the past, followed by calcite illuviation along later aridity as was also supported by Bayat et al. (2017) and Moghbeli et al. (2019). The compound clay-calcite pedo-feature is a proof of the formation of a polygenetic soil which has experienced different formation-development cycles due to climatic fluctuations.

Calcite coatings (Figs. 2a, d, m, o) are among the most important pedo-features which have formed through re-precipitation of illuviated calcium carbonates originated from upper horizons (Kemp et al., 2003). Dissolved calcium carbonate in the arid climate of the present time has formed infillings (Fig. 2d, o) in the pore spaces (Durand et al., 2010). Sarmast et al. (2019) reported coating, infilling and nodule pedo-features of calcite in soils of central Iran.

Meanwhile, lenticular and interlocked plates of gypsum (Fig. 2f) in By horizon of pedon 5 on mantled pediment were investigated. Soils of this pedon were not saline (Table 1) and were composed of high sand and coarse gravel contents. Large pore space content of the soil could facilitate lenticular formation of gypsum as was also supported by Amit and Yaloon (1996) and Farpoor et al. (2012) in Israel and central Iran, respectively. The same mechanism could also be attributed to the lenticular gypsum formation in Btky horizon of pedon 9 (Fig. 2k). Gypsum pendants (macroscopic form) and gypsum interlocked plates (microscopic form) in pedons 5 and 8 were attributed to coarse texture and high gravel content of pediments (Farpoor et al., 2003). Meanwhile, anhydrite was also formed in By1 horizon of pedon 7 (Fig. 2h), seemingly during gypsum transformation. The same results were reported by Aref (2003) and Sarmast et al. (2019) in soils of Egypt and central Iran, respectively.

Smectite, illite, and kaolinite clay minerals were found in pedon 3 (Table 2, Fig. 3d). Palygorskite and chlorite could not be formed or have been weathered in this position due to a xeric moisture regime. Smectite is the dominant clay mineral in this pedon (Table 2). Moreover, smectite, illite, chlorite, kaolinite, and palygorskite were found in soil (Btk1) and parent material (2Ck) of pedon 4 (Table 2. And Figs. 3e, f). The presence of the above-mentioned minerals in soils and parent material is a proof of inheritance origin from sedimentary formations which was also supported by Owliaie et al. (2018) for soils located on sedimentary formations of southwest Iran.

On the other hand, smectite, illite, chlorite, palygorskite, and kaolinite clay minerals were identified in other pedons (5-9) on this landform which were affected by igneous formations (Table 2, Figs. 3 g, h, i, j, k, l). No palygorskite was found in the igneous parent material (Fig. 2b), but calcic (Fig. 3i) and gypsic (Fig. 3j) horizons contained palygorskite. Geochemical conditions after the precipitation of calcium as calcium carbonate and gypsum in the arid climate of these pedons seem to have been favorable for palygorskite formation together with the increase of soluble Mg (Singer and Fine, 1989). A pedogenic origin for palygorskite in calcic (2Btk) horizon of pedon 6 (Fig. 4a) and gypsic horizon (Bty) of pedon 7 (Fig. 4b), both affected by igneous formations was proved using electron microscope observations. Preservation of palygorskite around calcite (Khademi and Mermut, 1998) and gypsum (Owliaie et al., 2018; Moazallahi and Farpoor, 2012; Khademi and Mermut, 1998) crystals in soils and sediments of central Iran were also reported. Moreover, the lack of palygorskite and chlorite in the modern topsoil of pedon 6 (Fig. 3h) could be attributed to the Halilrood River floods which may have caused their transformation to smectite

(Birkland, 1999). Smectite is the dominant mineral in the modern topsoil of pedon 6 (Table 2) which is another support for the above-mentioned discussion. Thus, both pedogenic and inherited origins for smectite in soils of the area are plausible (Sanjari et al., 2011).

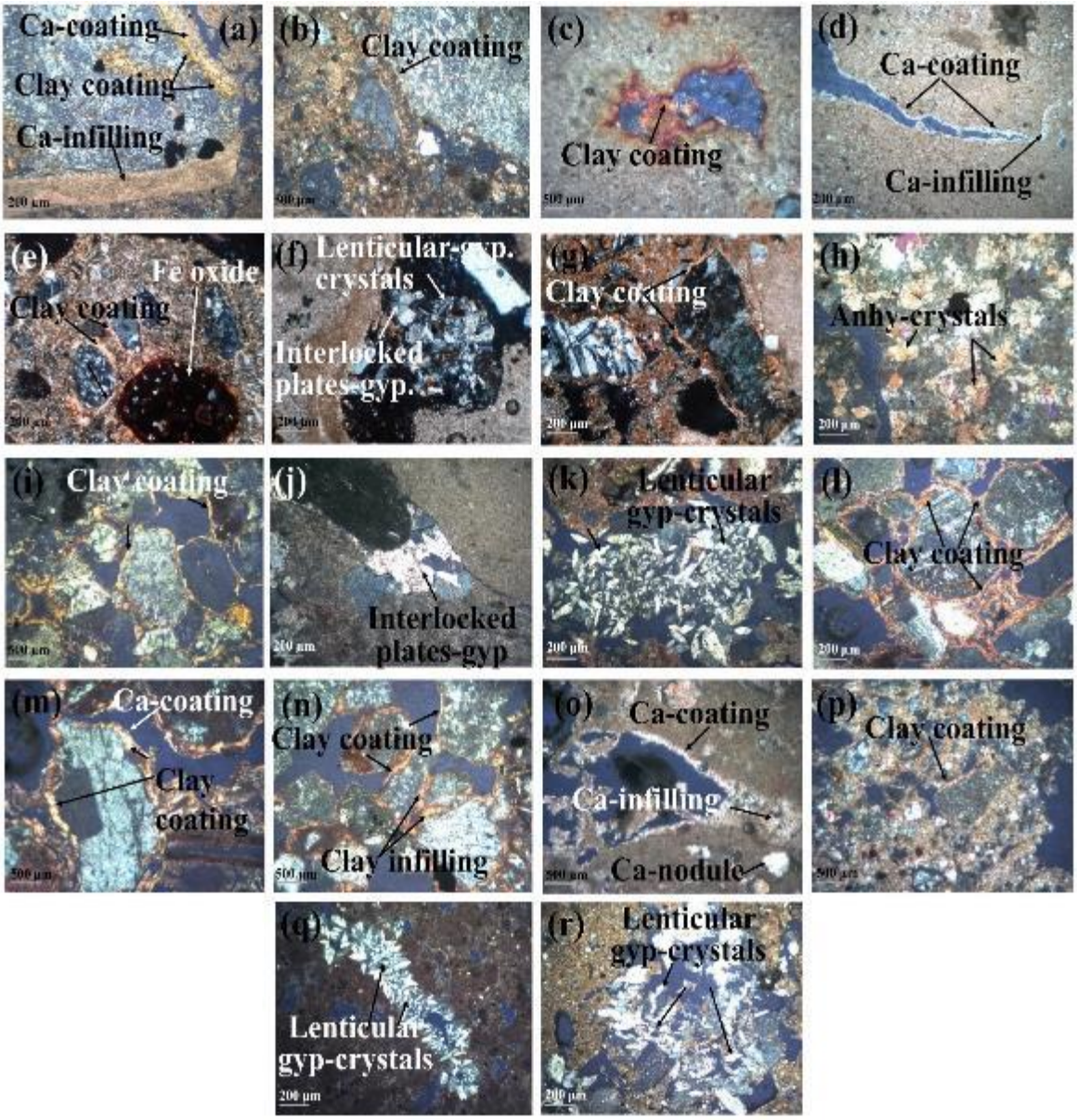

Figure 2. Thin sections of a) Clay and calcite coatings and dense incomplete calcite infilling in Btk horizon, pedon 3 (XPL), b) Clay coating in Btk2 horizon, pedon 4 (XPL), c) Clay coating in 2Btnkk1 horizon, pedon 4 (XPL), d) Coating and infilling of calcite in 2Btnkk1 horizon, pedon 4 (XPL), e) Clay coating and Fe oxide in Btk horizon, pedon 5 (XPL), f) Interlocked plates and lenticular forms of gypsum crystals in By horizon, pedon 5 (XPL), g) Clay coating in 2Btk horizon, pedon 6 (XPL),), h) Anhydrite crystals in By1 horizon, pedon 7 (XPL), i) Clay coating in Bty horizon, pedon 7 (XPL), j) Interlocked plates of gypsum in Bkyzn horizon, pedon 8 (XPL), k) Lenticular gypsum crystals in Btky horizon, pedon 9 (XPL), l) Clay coating in Btky horizon, pedon 9 (XPL), m) Clay and calcite coating in Btky horizon, pedon 9 (XPL), n) Coating and infilling of clay in Bk horizon, pedon 11 (XPL), o) Calcite coating, infilling, and nodule in Bk horizon, pedon 12 (XPL), p) Clay coating in Btk1 horizon, pedon 14 (XPL), q) Lenticular gypsum crystals in 3Btnzb1 horizon, pedon 16 (XPL), r) Lenticular gypsum crystals in Bz2 horizon, pedon 20 (XPL).

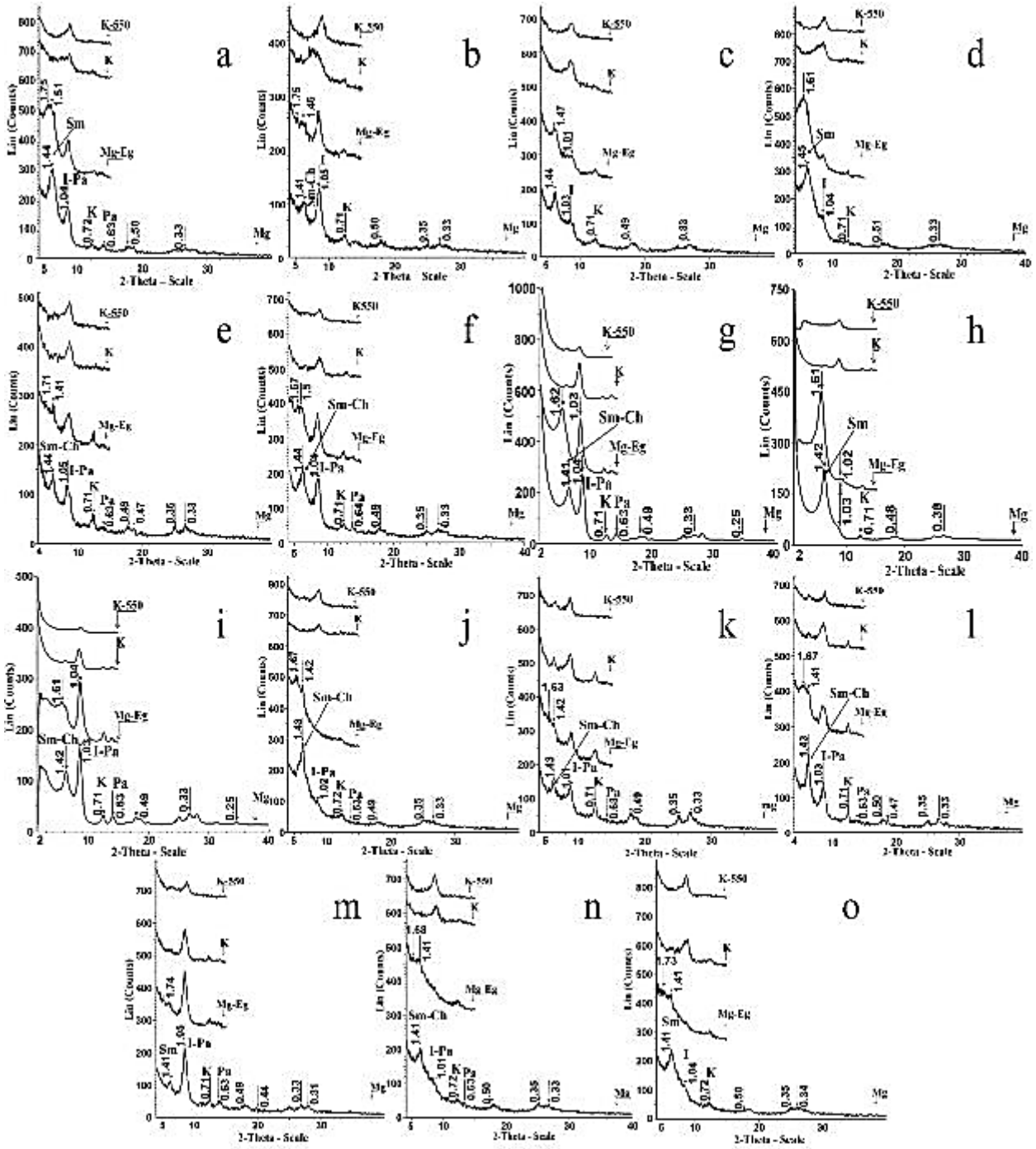

Figure 3. X-Ray diffractograms of the clay fraction, a) Bw1 horizon of pedon 1. b) R horizon of pedon 1, c) Bg1 horizon of pedon 2, d) 2Btk horizon of pedon 3, e) Btk1 horizon of pedon 4, f) 2Ck horizon of pedon 4, g) Btk horizon of pedon 5, h) Btn1 horizon of pedon 6, i) 2Btk horizon of pedon 6, j) Bty horizon of pedon 7, k) Bkyz1 horizon of pedon 8, l) Btky horizon of pedon 9, m) Btk1 horizon of pedon 14, n) Bz horizon of pedon 18, o) Btnz2 horizon of pedon 18. (Sm: Smectite, I: Illite, Pa: Palygorskite, Ch:Chlorite, Ka:Kaolinite. Mg=Mg saturated; Mg-Eg=Mg saturated with Ethylene glycol; K=K saturated; K-550=K saturated and heated to 550 °C).

Pedons 3 and 8 with the same parent material and geomorphology, but different soil moisture regime, have different soils. This is a proof for the important role of climate in soil formation compared to p (parent material) and r (relief) as soil forming factors in this part of the area. On the other hand, pedons 4 to 9 have the same geomorphology and climate, but parent material for pedon 4 (limestone) is different with other pedons (diorite). Results clearly show that somehow similar soils were formed in these pedons and limited differences in the suborder level were only observed. This in turn shows the high effective role of climate and geomorphology on soil formation in this landform.

3.4. Alluvial fan

Similar to mantled pediment, soils with various evolution were found in this landform. Soil moisture regime for alluvial fan is aridic which is why different soil evolutions (pedons 10-13) could be due to the difference in parent material (Table 1). Pedons 10 (east of Jiroft) and 13 (east of Iranshahr) located on young alluvial fan deposits and affected by granite formations showed very little soil development. The large distance from Neogene gypsiferous and saline formations on one hand, and the young Quaternary alluvial fan deposits on the other hand, are among the inhibiting factors controlling soil development in this geomorphic position. Moreover, the formation of bajada due to rainfall and the erosion of upland mountains in these two locations which are in the arid zone climate, could be evidence of a more humid climate in the past. The same results were also reported by Sarmast et al. (2017) in the study of alluvial fans in the central parts of Iran. Pedons 11 (with argillic and calcic horizons) and 12 (with calcic horizon) respectively affected by limestone and diabase (influenced by Mokran colored melange) parent materials showed soils with high and intermediate evolution located on old alluvial fan deposits. Micromorphological observations showed clay coatings and infillings in Btk horizon of pedon 11 (Fig. 2n) which are supporting proofs of argillic horizon formation. Calcite coating, infilling, and nodules were also determined in Bk horizon of pedon 12 (Fig. 2o). Formation of calcite nodule (Fig. 2o) in the Btk horizon of pedon 12 was due to dissolution/recrystallization of calcite in the groundmass. Sarmast et al. (2019) reported coating, infilling and nodule pedo-features of calcite in soils of central Iran. Entisols and Aridisols were formed on this geomorphic position.

Pedons 10 to 13 have the same geomorphology (alluvial fan) and climate (aridic soil moisture regime), but different parent material (igneous in pedons 10 and 13 vs. sedimentary in pedons 11

and 12). Formation of different soils is a proof of the role of parent material and time on soil formation when other soil formation factors are the same.

3.5. Rock pediment

This geomorphic position about 800 m asl and with an aridic soil moisture regime is affected by limestone together with shale and marl as parent material. Pedon 14 with argillic, calcic, and gypsic horizons were described and sampled on this position. Due to low SAR content (Table 1) and an aridic soil moisture regime, presence of argillic horizon similar to other arid parts of Jazmurian Watershed was attributed to the more available humidity of the past. That is why this soil was accounted as a paleosol. Removal of calcium carbonate from upper horizons with more humidity of the past (Bk horizon formation) followed by clay illuviation caused Btk horizon to be formed (Sanjari et al., 2011). Clay coating proved illuviation of clay and argillic horizon formation (Fig. 2p). Clay mineralogy of this soil was similar to mantled pediment position (Table 2, Fig. 3m). This soil was classified as Typic Calcigypsids.

3.6. Playa

Sodic clay flat (pedon 15), clay flat (pedon 16), fan delta (pedon 17), wet zone (pedon 18), puffy ground clay flat (pedon 19), and salt crust (pedon 20) geomorphic surfaces were found in playa about 360 m asl (Fig. 1). Salic and natric were the dominant horizons found in soils of this landform. High Na content caused clay dispersion and natric horizon formation in some pedons of this position as was also supported by Khormali et al. (2003). A modern and a buried paleosol were found (pedon 16) on clay flat geomorphic position. The modern soil with A and C horizons was a young soil affected by alluvial deposits, and 2Cz horizon showed the influence of aeolian deposits. Active wind erosion of the upland positions caused wind-blown deposits in this horizon. On the other hand, the buried soil is a developed soil with salic and natric horizons. Meanwhile, a non-saline (Table 1) Fluvisol (pedon 17) was found on fan delta geomorphic surface. Formation processes of fan delta position and the role of Halilrood River with a non-saline water, could be accounted for a non-saline soil to be formed in pedon 17.

Wet zone with an aquic soil moisture regime was located between alluvial fan and clay flat positions. The same geomorphic position was also reported by Farpoor et al. (2012) in Sirjan Playa. High electrical conductivity (EC) in the topsoil of puffy ground clay flat was attributed to evaporation and capillary water movement in this geomorphic position (Sanjari et al., 2011). The

thickness of salt polygons in the salt crust geomorphic position of the area was less than what reported for other playas (Sirjan, and Lut) of central Iran. Bampour seasonal river which has passed through evaporate formation of east side watershed contains more soluble salts compared to non-saline Halilrood River. Salt crust seems to be affected by Bampour River. Soils of this position were classified as Entisols and Aridisols (Table 1).

Lenticular gypsum crystals observed in 3Btnzb1 (pedon 16) and Bz2 (pedon 20) horizons. Soils in this position were fine textured with small pore spaces and high salinity (Table 1). The reason could be attributed to the NaCl content (Amit and Yaloon 1996) together with super saturation in respect to calcium sulfate in the fine pore spaces along time periods (Owliaie et al. 2006). Since gypsum content was not enough, gypsic horizon was not detected in these pedons.

Palygorskite was not detected in Btnz2 horizon of pedon 18 on wet zone geomorphic position (Fig. 3o). Due to high humidity content in this position (presence of an aquic soil moisture regime), transformation of palygorskite to smectite which was also reported by Khormali and Abtahi (2003) and Moghbeli et al. (2019) could not be neglected in this position. The dominance of smectite in this soil (Table 2) could be another support for the above-mentioned discussion. Since smectite was also determined (Fig. 3n) in the Bz horizon (near the soil surface), it seems that the detrital origin of smectite addition to the surface could be another plausible reason. The intense 0.63 nm peak of palygorskite was also due to the detrital transportation of broken palygorskite crystals from alluvial fan toward this position. That is why palygorskite in this geomorphic position is with a detrital origin which was also supported by split crystals observed using electron microscopy (Fig. 4). Farpoor and Irannejad (2013) and Khademi and Mermut (1998) also came to the same conclusion in Rafsanjan and Isfahan areas, central Iran.

Parent material and climate for pedons 15 to 20 are the same, but geomorphic surfaces have only changed which caused differences in order and suborder levels of soils formed in playa. This shows the role of topography (r) apart from climate and parent material in soil formation.

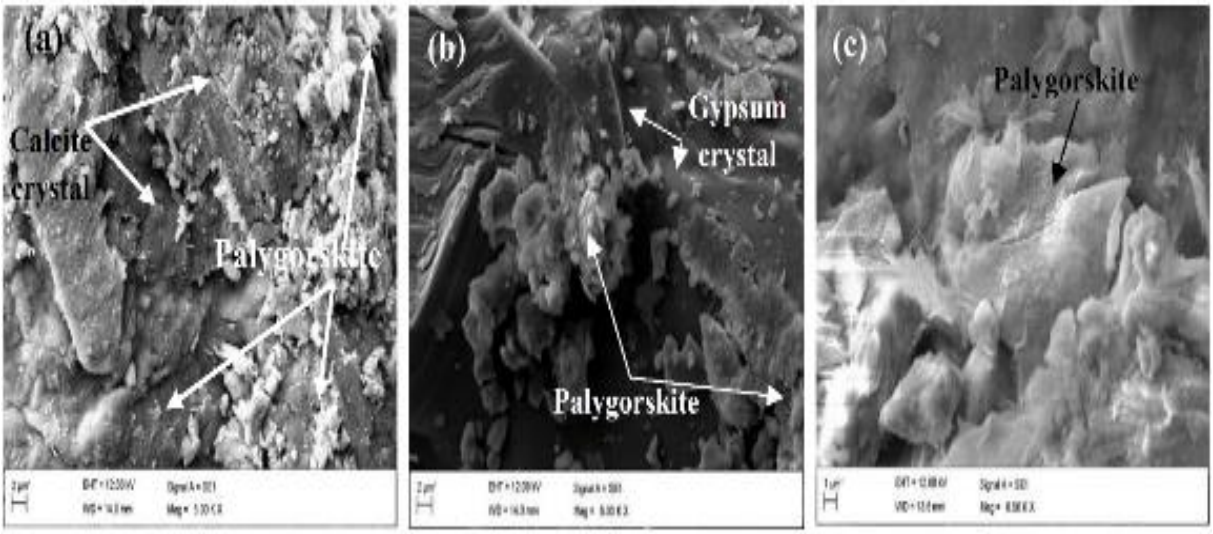

Figure 4. SEM micrographs of (a) palygorskite fibers on calcite crystal of the 2Btk horizon of pedon 4, (b) palygorskite fibers on gypsum crystal of the Bty horizon of pedon 5, (c) palygorskite broken fibers of the Bzn horizon of pedon 18.

4. Conclusions

Various soils were formed through the climolithotoposequence studied in Jazmurian Watershed. The electrical conductivity content increased toward playa and the maximum EC content of 222.2 dS/m was determined in salt crust geomorphic position of playa. Soil evolution was highly depended on parent material and the decreasing trend of soil evolution (granite-young alluvial fan deposits< playa deposits< limestone-old alluvial fan deposits< andesite- diorite) was found in the area. Soils were classified as Mollisols, Alfisols, Aridisols, Inceptisols, and Entisols. Different pedofeatures in argillic and calcic horizons in both xeric and aridic soil moisture regimes of the area were found. However, pedo-features related to gypsic and anhydritic horizons were only found in the arid parts of the transect. The presence of a more humid paleoclimate in the history of the area which was supported by clay coatings was proved by argillic horizons formed in the arid parts of the area. A dispersed clay coating was found in natric horizons. Smectite, illite, chlorite, palygorskite, and kaolinite clay minerals were identified. Palygorskite was only found in the arid parts of the area and pedogenic and inherited origins were respectively found in igneous and sedimentary affected soils. Palygorskite in piedmont plain about 3620 m asl was with an aeolian origin. Illite and chlorite clay minerals were identified in both sedimentary and igneous parent materials with an inherited origin, but lack of these minerals in some of the soils under study could be attributed to their transformation to smectite which was also supported by smectite peak

intensity in such soils. That is why both inherited and transformed (from illite, chlorite, and palygorskite) sources of smectite in the area were plausible.

Results of the study emphasized on the more effective role of climate and relief on soil formation compared to parent material. The role of climate, alone or together with relief on soil formation and evolution in pedons 1 to 9 seems to be greater than that of parent material. Since climate and relief have not changed along pedons 10 to 14, parent material affected soil formation and evolution. Moreover, relief has controlled soil formation and development in pedons 15 to 20 as climate and parent material were the same in these pedons. The hypothesis regarding the effects of climate, topography, and parent material soil forming factors on soil formation and development (climolithotoposequence) in the area was clearly proved.

References

Amit. R., Yaalon, A. D., 1996. The micromorphology of gypsum and halite in reg soils: The Negev desert, Israel. Earth Surf. Proc. Landf. 21, 1127–1143.

Aref, M. A. M., 2003. Classification and depositional environments of Quaternary pedogenic gypsum crusts (gypcrete) from east of the Fayum Depression, Egypt. Sed. Geol. 155(1), 87–108.

Artieda, O., Herrero, J., Drohan, P. J., 2006. Refinement of the differential water loss method for gypsum determination in soils. Soil Sci. Soc. of Amer. J. 70, 1932–1935.

Badia, D., Buendia-Garcia, L., Longares-Aladrén, L., Marti-Dalmau, C., Peña-Monné, J., González-Pérez, J., Gómez-Garcia, D., 2020. Soil-geomorphology relationships determine the distribution of the main subalpine grasslands in the Central Pyrenees (NE-Spain). Sci. of the Total Environ. 734, 139121.

Banaie, M. H., 1998. Soil Moisture and Temperature Regimes Map of Iran. Iran: Soil and Water Res. Institute.

Bayat, O., Karimzadeh, H., Karimi, A., Karimian Eghbal, M., Khademi, H., 2017. Paleoenvironment of geomorphic surfaces of an alluvial fan in the eastern Isfahan, Iran, in the light of micromorphology and clay mineralogy. Arab. J. of Geosci. 10, 91

Birkeland, P. W., 1999. Soils and Geomorphology. New York: Oxford University Press.

Bower, C. A., Hatcher, J. T., 1966. Simultaneous determination of surface area and cation exchange capacity. Soil Sci. Soc. of Amer. J. 30, 525–527.

Durand, N., Monger, H. C., Canti, M. G., 2010. Calcium carbonate features. In: G. Stoops, V. Marcelino, & F. Mees (Eds.), Interpretation of micromorphological features of soils and regoliths. Amsterdam, Netherlands (pp. 149–182). Elsevier.

Egli, M., Merkli Ch., Sartori, G., Mirabella, A., Plotze, M., 2008. Weathering, mineralogical evolution and soil organic matter along a Holocene soil toposequence developed on carbonate-rich materials. Geomorphology 97, 675–696.

Elliott, P.E., Dorhan, P.J., 2009. Clay accumulation and argillic-horizon development as influenced by aeolian vs. local parent material on quartzite and limestone-derived alluvial fans. Geoderma 151, 98-108.

Farpoor, M. H., Eghbal, M. K., Khademi, H., 2003. Genesis and micromorphology of saline and gypsiferous Aridisols on different geomorphic surfaces in Nough area, Rafsanjan. J. of Sci. & Tech. of Agri. & Natur. Resour. 7, 71–93. (in Persian with English abstract)

Farpoor, M. H., Neyestani, M., Eghbal, M. K., Esfandiarpour Borujeni, I., 2012. Soil–geomorphology relationships in Sirjan playa, south-central Iran. Geomorphology 138(1), 223–230.

Farpoor, M. H., Irannejad, M., 2013. Soil genesis and clay mineralogy on Aliabbas River alluvial fan, Kerman Province. Arab. J. of Geosci. 6(3), 921–928.

Gee, G. W., Bauder, J. W., 1986. Particle size analysis. In: A. Klute (Eds.), Methods of Soil Analysis, Agronomy Monograph, Vol 9 (pp. 383–411). Madison, WI: American Society of Agronomy/Soil Science Society of America.

Graham R.C., O'Geen A.T., 2010. Soil mineralogy trends in California landscapes. Geoderma 154, 418–437.

Jackson, M. L., 1975. Soil Chemical Analysis-advanced Course. Madison, WI: University of Wisconsin College of Agriculture, Department of Soil Science.

Johns, W.D., Grim, R.E., Bradly, W.F., 1954. Quantitative Estimation of Clay Minerals by Diffraction Methods. J. Sed. Petrol. 24, 242-251.

Kemp, R. A., Tomas, P. S., Sayago, J. M., Debyshire, E., King, M., Wagner, L., 2003. Micromorphology OSL dating of the basalt part of the loess-paleosol sequence at La Mesuda in Tucuman province, northwest Argentina. Quarter. Int. 106–107, 111–117.

Kittrick, J. A., Hope, E. W., 1963. A procedure for the particle-size separation of soils for X-ray diffraction analysis. Soil Sci. *96(5)*, 319–325.

Khademi, H., Mermut, A. R., 1998. Source of palygorskite in gypsiferous Aridisols and associated sediments from central Iran. Clay Miner. 33(4), 561–578.

Khademi, H., Mermut, A. R., 2003. Micromorphology and classification of Argids and associated gypsiferous Aridisols from central Iran. Catena 54, 439–455.

Khormali, F., Abtahi, A., 2003. Origin and distribution of clay minerals in calcareous arid and semiarid soils of Fars Province, southern Iran. Clay Miner. 38(4), 511–527.

Khormali, F., Abtahi, A., Mahmoodi, S., Stoops, G., 2003. Argillic horizon development in calcareous soils of arid and semiarid regions of southern Iran. Catena 53(3), 273–301.

Krinsley, D. B., 1970. A Geomorphological and Paleoclimatological Study of the Playas of Iran. Washington DC: Geological Survey, United States Department of Interior.

Moazallahi, M., Farpoor, M. H., 2012. Soil genesis and clay mineralogy along the xeric aridic climotoposequence, South central Iran. J. of Agri. Sci. and Tech. 14, 683–696.

Moghbeli, M., Owliaie, H. R., Sanjari, S., Adhami, E., 2019. Genetic Study of Soil-Landscape Relationship in Arid Region of Faryab, Kerman Province. J. of Water and Soil 33(2), 333–347. (in Persian with English abstract)

Mohammadi, A., 2011. Sedimentology and sedimentary geochemistry of Jazmuriyan Playa. Arid Biom Scientific and Res. J. 1(1): 68–78. (in Persian with English abstract)

Monafi, S.H. (2010). Mineralogical Evidence of Climate Change in some Semiarid Soils of SouthernUrmia, Iran. Soil Science Agrochem. and Ecol. 4, 17-24.

Namaki, L., 2003. Analysis of Makran aeromagnetic data. Iran: University of Tehran, Institute of Geophysics. (in Persian with English abstract)

Nelson, R. E., 1982. Carbonate and Gypsum. In: A. L. Page, R. H. Miller, & D. R. Keeney (Eds.), Methods of Soil Analysis. Part II. 2nd ed., Agronomy Monogarph, Vol 9. Madison, WI: American Society of Agronomy/Soil Science Society of America (pp. 181–196).

Nelson, D. W., Sommers, L. E., 1982. Total Carbon, Organic Carbon and Organic Matter. In: A. L. Page, R. H. Miller, & D. R. Keeney (Eds.), Methods of Soil Analysis. Part II. 2nd ed., Agronomy Monogarph, Vol 9. Madison, WI: American Society of Agronomy/Soil Science Society of America (pp. 539–577).

O'Geen, A.T., Hobson, W.A., Dahlgren, R.A., Kelly, D.B., 2008. Evaluations of soil properties and hydric soil indicators for vernal pool catenas in California. Soil Sci. Soc. of Amer. J. 72: 727–740.

Owliaie, H. R., Abtahi, A., Heck, R. J., 2006. Pedogenesis and clay mineralogical investigation of soils formed on gypsiferous and calcareous materials on a transect, Southwestern Iran. Geoderma 134, 62–81.

Owliaie, H. R., Adhami, E., Najafi Ghiri, M., Shakeri, S., 2018. Pedological Investigation of a Litho-Toposequence in a Semi-Arid Region of Southwestern Iran. Euras. Soil Sci. 51(12), 1447–1461.

Paquet, H., Millot, C., 1972. Geochemical evolution of clay minerals in the weathered products and soils of Mediterranean climates. Proceedings of the 9th International Clay Conference, Madrid, Spain (pp. 199–202).

Phillips, J., Turkingtan, A.V., Marine, D.A., 2008. Weathering and vegetation affection early stages of soil formation. Catena 72, 21-28.

Saez, A., Ingles, M., Cabrera, L., Heras, A., 2003. Tectonic Paleoenvironmental Forcing of Clay-Mineral Assemblages in Non-Marine Setting: The Oligocene-Miocene Aspontes Basin (Spain). Sed. Geol. 159: 305-324.

Sanjari, S., Farpoor, M. H., Eghbal, M. K., Esfandiarpoor Boroujeni, I., 2011. Genesis, micromorphology and clay mineralogy of soils located on different geomorphic surfaces in Jiroft area. J. of Water and Soil 25(2), 411–425. (in Persian with English abstract)

Sanjari, S., Farpoor, M. H., Esfandiarpoor Boroujeni, I., Eghbal, M. K., 2012. Micromorphology and clay mineralogy comparison of past and present soils in Jiroft area. J. of Water and Soil Sci. 15(58): 173-185 (in Persian with English abstract).

Sarmast, M., Farpoor, M. H., Esfandiarpour Boroujeni, I., 2017. Soil and desert varnish development as indicators of landform evolution in central Iranian deserts. Catena 149, 98–109.

Sarmast, M., Farpoora, M. H., Jafaria, A., Esfandiarpour Borujeni, I., 2019. Tracing environmental changes and paleoclimate using the micromorphology of soils and desert varnish in central Iran. Desert 24(2), 331–353.

Schoeneberger, P. J., Wysocki, D. A., Benham, E. C., 2012. Field Book for Describing and Sampling Soils. Lincoln, NE: Natural Resources Conservation Service, National Soil Survey Center.

Singer, A. (1989). Palygorskite and Sepiolite Group Minerals. In J.B. Dixon, & D.G. Schulze (Eds.), Soil Mineralogy with Environmental Applications (pp. 556-580). Madison, Wisconsin, USA: Soil Science Society of America.

Singer, M.J., Fine, P., 1989. Pedogenic factors affecting magnetic susceptibility of California soils. Soil Sci. Soc. of Amer. J. 53, 1119-1127.

Soil Survey Staff, 2022. Keys to Soil Taxonomy, 13th Edition. Washington, D.C: United States Department of Agriculture and Natural Resources Conservation Service.

Stoops, G., 2003. Guidelines for the Analysis and Description of Soil and Regolith Thin Sections. Madison, WI: Soil Science Society of America.

Wilson, M. A., Shahid, S. A., Abdelfattah, M. A., Kelley, J. A., Thomas, J. E., 2013. Anhydrite formation on the Coastal Sabkha of Abu Dhabi, United Arab Emirates. In: S. A. Shahid, F. K. Taha, & M. A. Abdelfattah (Eds.). Developments in Soil Classification, Land Use Planning and Policy Implications: Innovative Thinking of Soil Inventory for Land Use Planning and Management of Land Resources (pp. 175–201). Netherlands: Springer SBM Publishing.

Wilson, S.G., Lambert, J.-J., Nanzyo, M., Dahlgren, R.A., 2017. Soil genesis and mineralogy across a volcanic lithosequence. Geoderma 285, 301–312. https://linkinghub.elsevier.com/retrieve/pii/S001670611630430X.

Yousefifard, M., Ayoubi, S., Poch, R.M., Jalalian, A., Khademi, H., Khormali, F., 2015. Clay transformation and pedogenic calcite formation on a lithosequence of igneous rocks in northwestern Iran. Catena 133, 186–197.